A measurement of $|V_{cb}|$ from $\overline{B}^0 \to D^{*+} l^- \overline{\nu}_l$

D. Buskulic, D. Casper, I. de Bonis, D. Decamp, P. Ghez, C. Goy, J.P. Lees, M.N. Minard, P. Odier, B. Pietrzyk, et al.

CERN-PPE/95-094
29 June 1995

A Measurement of $|V_{cb}|$ from $\overline{B}^0 \to D^{*+}\ell^-\overline{\nu}_\ell$

The ALEPH Collaboration

Abstract

From approximately 3 million hadronic decays of Z bosons recorded with the ALEPH detector at LEP, a sample of 410 ± 32 $\overline{B}^0 \to D^{*+}\ell^-\overline{\nu}_\ell$ candidates is selected, where ℓ is either an electron or a muon. The differential decay rate $d\Gamma(\overline{B}^0 \to D^{*+}\ell^-\overline{\nu}_\ell)/d\omega$ from this sample is fitted, yielding a value for the product of the CKM matrix element $|V_{cb}|$ and the normalisation of the decay form factor at the point of zero recoil of the D^{*+} meson $\mathcal{F}(\omega = 1)|V_{cb}| = (31.4 \pm 2.3_{stat} \pm 2.5_{syst}) \times 10^{-3}$. A value for $|V_{cb}|$ is extracted using theoretical calculations of the form factor normalisation, with the result $|V_{cb}| = (34.5 \pm 2.5_{stat} \pm 2.7_{syst} \pm 1.5_{theory}) \times 10^{-3}$. From the integrated spectrum, the measured branching fraction is $Br(\overline{B}^0 \to D^{*+}\ell^-\overline{\nu}_\ell) = (5.18 \pm 0.30_{stat} \pm 0.62_{syst})\%$.

(Submitted to *Physics Letters B*)

See following pages for the list of authors

The ALEPH Collaboration

D. Buskulic, D. Casper, I. De Bonis, D. Decamp, P. Ghez, C. Goy, J.-P. Lees, A. Lucotte, M.-N. Minard, P. Odier, B. Pietrzyk

Laboratoire de Physique des Particules (LAPP), IN^{2}P^3-CNRS, 74019 Annecy-le-Vieux Cedex, France

F. Ariztizabal, M. Chmeissani, J.M. Crespo, I. Efthymiopoulos, E. Fernandez, M. Fernandez-Bosman, V. Gaitan, Ll. Garrido,[15] M. Martinez, S. Orteu, A. Pacheco, C. Padilla, F. Palla, A. Pascual, J.A. Perlas, F. Sanchez, F. Teubert

Institut de Fisica d'Altes Energies, Universitat Autonoma de Barcelona, 08193 Bellaterra (Barcelona), Spain[7]

A. Colaleo, D. Creanza, M. de Palma, A. Farilla, G. Gelao, M. Girone, G. Iaselli, G. Maggi,[3] M. Maggi, N. Marinelli, S. Natali, S. Nuzzo, A. Ranieri, G. Raso, F. Romano, F. Ruggieri, G. Selvaggi, L. Silvestris, P. Tempesta, G. Zito

Dipartimento di Fisica, INFN Sezione di Bari, 70126 Bari, Italy

X. Huang, J. Lin, Q. Ouyang, T. Wang, Y. Xie, R. Xu, S. Xue, J. Zhang, L. Zhang, W. Zhao

Institute of High-Energy Physics, Academia Sinica, Beijing, The People's Republic of China[8]

G. Bonvicini, D.G. Cassel,[27] M. Cattaneo, P. Comas, P. Coyle, H. Drevermann, A. Engelhardt, R.W. Forty, M. Frank, R. Hagelberg, J. Harvey, R. Jacobsen,[24] P. Janot, B. Jost, J. Knobloch, I. Lehraus, C. Markou,[23] E.B. Martin, P. Mato, H. Meinhard, A. Minten, R. Miquel, K. Moffeit,[28] T. Oest, P. Palazzi, J.R. Pater,[29] J.-F. Pusztaszeri, F. Ranjard, P. Rensing, L. Rolandi, D. Schlatter, M. Schmelling, O. Schneider, W. Tejessy, I.R. Tomalin, A. Venturi, H. Wachsmuth, W. Wiedenmann, T. Wildish, W. Witzeling, J. Wotschack

European Laboratory for Particle Physics (CERN), 1211 Geneva 23, Switzerland

Z. Ajaltouni, M. Bardadin-Otwinowska,[2] A. Barres, C. Boyer, A. Falvard, P. Gay, C. Guicheney, P. Henrard, J. Jousset, B. Michel, S. Monteil, J-C. Montret, D. Pallin, P. Perret, F. Podlyski, J. Proriol, J.-M. Rossignol, F. Saadi

Laboratoire de Physique Corpusculaire, Université Blaise Pascal, IN^{2}P^3-CNRS, Clermont-Ferrand, 63177 Aubière, France

T. Fearnley, J.B. Hansen, J.D. Hansen, J.R. Hansen, P.H. Hansen, B.S. Nilsson

Niels Bohr Institute, 2100 Copenhagen, Denmark[9]

A. Kyriakis, E. Simopoulou, I. Siotis, A. Vayaki, K. Zachariadou

Nuclear Research Center Demokritos (NRCD), Athens, Greece

A. Blondel,[21] G. Bonneaud, J.C. Brient, P. Bourdon, L. Passalacqua, A. Rougé, M. Rumpf, R. Tanaka, A. Valassi,[33] M. Verderi, H. Videau

Laboratoire de Physique Nucléaire et des Hautes Energies, Ecole Polytechnique, IN^{2}P^3-CNRS, 91128 Palaiseau Cedex, France

D.J. Candlin, M.I. Parsons

Department of Physics, University of Edinburgh, Edinburgh EH9 3JZ, United Kingdom[10]

E. Focardi, G. Parrini

Dipartimento di Fisica, Università di Firenze, INFN Sezione di Firenze, 50125 Firenze, Italy

M. Corden, M. Delfino,[12] C. Georgiopoulos, D.E. Jaffe

Supercomputer Computations Research Institute, Florida State University, Tallahassee, FL 32306-4052, USA [13,14]

A. Antonelli, G. Bencivenni, G. Bologna,[4] F. Bossi, P. Campana, G. Capon, V. Chiarella, G. Felici, P. Laurelli, G. Mannocchi,[5] F. Murtas, G.P. Murtas, M. Pepe-Altarelli

Laboratori Nazionali dell'INFN (LNF-INFN), 00044 Frascati, Italy

S.J. Dorris, A.W. Halley, I. ten Have,[6] I.G. Knowles, J.G. Lynch, W.T. Morton, V. O'Shea, C. Raine, P. Reeves, J.M. Scarr, K. Smith, M.G. Smith, A.S. Thompson, F. Thomson, S. Thorn, R.M. Turnbull

Department of Physics and Astronomy, University of Glasgow, Glasgow G12 8QQ,United Kingdom[10]

U. Becker, O. Braun, C. Geweniger, G. Graefe, P. Hanke, V. Hepp, E.E. Kluge, A. Putzer, B. Rensch, M. Schmidt, J. Sommer, H. Stenzel, K. Tittel, S. Werner, M. Wunsch

Institut für Hochenergiephysik, Universität Heidelberg, 69120 Heidelberg, Fed. Rep. of Germany[16]

R. Beuselinck, D.M. Binnie, W. Cameron, D.J. Colling, P.J. Dornan, N. Konstantinidis, L. Moneta, A. Moutoussi, J. Nash, G. San Martin, J.K. Sedgbeer, A.M. Stacey

Department of Physics, Imperial College, London SW7 2BZ, United Kingdom[10]

G. Dissertori, P. Girtler, E. Kneringer, D. Kuhn, G. Rudolph

Institut für Experimentalphysik, Universität Innsbruck, 6020 Innsbruck, Austria[18]

C.K. Bowdery, T.J. Brodbeck, P. Colrain, G. Crawford, A.J. Finch, F. Foster, G. Hughes, T. Sloan, E.P. Whelan, M.I. Williams

Department of Physics, University of Lancaster, Lancaster LA1 4YB, United Kingdom[10]

A. Galla, A.M. Greene, K. Kleinknecht, G. Quast, J. Raab, B. Renk, H.-G. Sander, R. Wanke, C. Zeitnitz

Institut für Physik, Universität Mainz, 55099 Mainz, Fed. Rep. of Germany[16]

J.J. Aubert, A.M. Bencheikh, C. Benchouk, A. Bonissent,[21] G. Bujosa, D. Calvet, J. Carr, C. Diaconu, F. Etienne, M. Thulasidas, D. Nicod, P. Payre, D. Rousseau, M. Talby

Centre de Physique des Particules, Faculté des Sciences de Luminy, IN^{2}P^3-CNRS, 13288 Marseille, France

I. Abt, R. Assmann, C. Bauer, W. Blum, D. Brown,[24] H. Dietl, F. Dydak,[21] G. Ganis, C. Gotzhein, K. Jakobs, H. Kroha, G. Lütjens, G. Lutz, W. Männer, H.-G. Moser, R. Richter, A. Rosado-Schlosser, S. Schael, R. Settles, H. Seywerd, U. Stierlin,[2] R. St. Denis, G. Wolf

Max-Planck-Institut für Physik, Werner-Heisenberg-Institut, 80805 München, Fed. Rep. of Germany[16]

R. Alemany, J. Boucrot, O. Callot, A. Cordier, F. Courault, M. Davier, L. Duflot, J.-F. Grivaz, Ph. Heusse, M. Jacquet, D.W. Kim,[19] F. Le Diberder, J. Lefrançois, A.-M. Lutz, G. Musolino, I. Nikolic, H.J. Park, I.C. Park, M.-H. Schune, S. Simion, J.-J. Veillet, I. Videau

Laboratoire de l'Accélérateur Linéaire, Université de Paris-Sud, IN^{2}P^3-CNRS, 91405 Orsay Cedex, France

D. Abbaneo, P. Azzurri, G. Bagliesi, G. Batignani, S. Bettarini, C. Bozzi, G. Calderini, M. Carpinelli, M.A. Ciocci, V. Ciulli, R. Dell'Orso, R. Fantechi, I. Ferrante, L. Foà,[1] F. Forti, A. Giassi, M.A. Giorgi, A. Gregorio, F. Ligabue, A. Lusiani, P.S. Marrocchesi, A. Messineo, G. Rizzo, G. Sanguinetti, A. Sciabà, P. Spagnolo, J. Steinberger, R. Tenchini, G. Tonelli,[26] G. Triggiani, C. Vannini, P.G. Verdini, J. Walsh

Dipartimento di Fisica dell'Università, INFN Sezione di Pisa, e Scuola Normale Superiore, 56010 Pisa, Italy

A.P. Betteridge, G.A. Blair, L.M. Bryant, F. Cerutti, Y. Gao, M.G. Green, D.L. Johnson, T. Medcalf, Ll.M. Mir, P. Perrodo, J.A. Strong

Department of Physics, Royal Holloway & Bedford New College, University of London, Surrey TW20 OEX, United Kingdom[10]

V. Bertin, D.R. Botterill, R.W. Clifft, T.R. Edgecock, S. Haywood, M. Edwards, P. Maley, P.R. Norton, J.C. Thompson

Particle Physics Dept., Rutherford Appleton Laboratory, Chilton, Didcot, Oxon OX11 OQX, United Kingdom[10]

B. Bloch-Devaux, P. Colas, H. Duarte, S. Emery, W. Kozanecki, E. Lançon, M.C. Lemaire, E. Locci, B. Marx, P. Perez, J. Rander, J.-F. Renardy, A. Rosowsky, A. Roussarie, J.-P. Schuller, J. Schwindling, D. Si Mohand, A. Trabelsi, B. Vallage

CEA, DAPNIA/Service de Physique des Particules, CE-Saclay, 91191 Gif-sur-Yvette Cedex, France[17]

R.P. Johnson, H.Y. Kim, A.M. Litke, M.A. McNeil, G. Taylor

Institute for Particle Physics, University of California at Santa Cruz, Santa Cruz, CA 95064, USA[22]

A. Beddall, C.N. Booth, R. Boswell, S. Cartwright, F. Combley, I. Dawson, A. Koksal, M. Letho, W.M. Newton, C. Rankin, L.F. Thompson

Department of Physics, University of Sheffield, Sheffield S3 7RH, United Kingdom[10]

A. Böhrer, S. Brandt, G. Cowan, E. Feigl, C. Grupen, G. Lutters, J. Minguet-Rodriguez, F. Rivera,[25] P. Saraiva, L. Smolik, F. Stephan, P. van Gemmeren

Fachbereich Physik, Universität Siegen, 57068 Siegen, Fed. Rep. of Germany[16]

M. Apollonio, L. Bosisio, R. Della Marina, G. Giannini, B. Gobbo, F. Ragusa[20]

Dipartimento di Fisica, Università di Trieste e INFN Sezione di Trieste, 34127 Trieste, Italy

J. Rothberg, S. Wasserbaech

Experimental Elementary Particle Physics, University of Washington, WA 98195 Seattle, U.S.A.

S.R. Armstrong, L. Bellantoni,[32] P. Elmer, Z. Feng, D.P.S. Ferguson, Y.S. Gao, S. González, J. Grahl, J.L. Harton,[30] O.J. Hayes, H. Hu, P.A. McNamara III, J.M. Nachtman, W. Orejudos, Y.B. Pan, Y. Saadi, M. Schmitt, I.J. Scott, V. Sharma,[31] J.D. Turk, A.M. Walsh, Sau Lan Wu, X. Wu, J.M. Yamartino, M. Zheng, G. Zobernig

Department of Physics, University of Wisconsin, Madison, WI 53706, USA[11]

[1]Now at CERN, 1211 Geneva 23, Switzerland.
[2]Deceased.
[3]Now at Dipartimento di Fisica, Università di Lecce, 73100 Lecce, Italy.
[4]Also Istituto di Fisica Generale, Università di Torino, Torino, Italy.
[5]Also Istituto di Cosmo-Geofisica del C.N.R., Torino, Italy.
[6]Now at TSM Business School, Enschede, The Netherlands.
[7]Supported by CICYT, Spain.
[8]Supported by the National Science Foundation of China.
[9]Supported by the Danish Natural Science Research Council.
[10]Supported by the UK Particle Physics and Astronomy Research Council.
[11]Supported by the US Department of Energy, contract DE-AC02-76ER00881.
[12]On leave from Universitat Autonoma de Barcelona, Barcelona, Spain.
[13]Supported by the US Department of Energy, contract DE-FG05-92ER40742.
[14]Supported by the US Department of Energy, contract DE-FC05-85ER250000.
[15]Permanent address: Universitat de Barcelona, 08208 Barcelona, Spain.
[16]Supported by the Bundesministerium für Forschung und Technologie, Fed. Rep. of Germany.
[17]Supported by the Direction des Sciences de la Matière, C.E.A.
[18]Supported by Fonds zur Förderung der wissenschaftlichen Forschung, Austria.
[19]Permanent address: Kangnung National University, Kangnung, Korea.
[20]Now at Dipartimento di Fisica, Università di Milano, Milano, Italy.
[21]Also at CERN, 1211 Geneva 23, Switzerland.
[22]Supported by the US Department of Energy, grant DE-FG03-92ER40689.
[23]Now at University of Athens, 157-71 Athens, Greece.
[24]Now at Lawrence Berkeley Laboratory, Berkeley, CA 94720, USA.
[25]Partially supported by Colciencias, Colombia.
[26]Also at Istituto di Matematica e Fisica, Università di Sassari, Sassari, Italy.
[27]Now at Newman Laboratory, Cornell University, Ithaca, NY 14853, U.S.A.
[28]Now at SLAC, Stanford University, Stanford, CA 94309, U.S.A.
[29]Now at Schuster Laboratory, University of Manchester, Manchester M13 9PL, UK.
[30]Now at Colorado State University, Fort Collins, CO 80523, USA.
[31]Now at University of California at San Diego, La Jolla, CA 92093, USA.
[32]Now at Fermi National Accelerator Laboratory, Batavia, IL 60510, USA.
[33]Supported by the Commission of the European Communities, contract ERBCHBICT941234.

1 Introduction

Recent developments [1, 2, 3, 4] in Heavy Quark Effective Theory (HQET) have raised hopes for a precise and model-independent measurement of $|V_{\rm cb}|$ using exclusive decays such as $\overline{\rm B}^0 \to {\rm D}^{*+}\ell^-\overline{\nu}_\ell$. In the massless lepton limit, there are three form factors in this decay. HQET relates these form factors to one universal function. The expression for the differential partial width for $\overline{\rm B}^0 \to {\rm D}^{*+}\ell^-\overline{\nu}_\ell$ decay is [4]:

$$\begin{aligned}\frac{d\Gamma}{d\omega} &= \frac{1}{\tau_{\rm B^0}}\frac{d\,{\rm Br}(\overline{\rm B}^0 \to {\rm D}^{*+}\ell^-\overline{\nu}_\ell\ )}{d\omega} \\ &= \frac{G_{\rm F}^2}{48\pi^3} m_{\rm D^{*+}}^3 (m_{\rm B^0} - m_{\rm D^{*+}})^2 \mathcal{F}^2(\omega) |V_{\rm cb}|^2 \sqrt{\omega^2-1} \\ &\quad \times \left[4\omega(\omega+1)\frac{1-2\omega r + r^2}{(1-r)^2} + (\omega+1)^2 \right] , \end{aligned} \tag{1}$$

where $r = m_{\rm D^{*+}}/m_{\rm B^0}$ and ω is the scalar product of the four-velocities of the $\overline{\rm B}^0$ and ${\rm D}^{*+}$ mesons: $\omega = v_{\rm B^0} \cdot v_{\rm D^{*+}}$. The unknowns are $|V_{\rm cb}|$ and $\mathcal{F}(\omega)$. The function $\mathcal{F}(\omega)$ is not specified by HQET but its magnitude at $\omega = 1$ is normalized to one in the heavy quark limit. The experimental data near this point are statistically deficient due to vanishing phase space. Consequently, in this method $\mathcal{F}(1)|V_{\rm cb}|$ is measured from $d\Gamma/d\omega$ by extrapolation, and a value for $|V_{\rm cb}|$ is derived using theoretical estimations of $\mathcal{F}(1)$ [5, 6, 7].

All such measurements of $|V_{\rm cb}|$ have come from the ARGUS and CLEO experiments [8, 9]. At the $\Upsilon(4S)$ resonance, the pion from the ${\rm D}^*$ decay has a typical momentum of about $0.1\,{\rm GeV}/c$ in the lab frame and is even softer in the vicinity of $\omega = 1$. As a result, the efficiency for reconstructing charged pions from ${\rm D}^{*+}$ decays is low, and the combinatorial background for neutral pions from ${\rm D}^{*0}$ decays is significant.

At the Z resonance, the B hadrons are produced with a large and variable boost of $\beta\gamma \approx 6$. Consequently, the pion from the ${\rm D}^{*+}$ decay has an average momentum of about $1\,{\rm GeV}/c$ and can be reconstructed with a high efficiency. This feature of B meson production allows access to the entire $d\Gamma/d\omega$ spectrum in $\overline{\rm B}^0 \to {\rm D}^{*+}\ell^-\overline{\nu}_\ell$ decays with similar efficiency. This advantage is offset by the need to reconstruct the B meson momentum four-vector on an event by event basis. The B meson four-momentum in $\overline{\rm B}^0 \to {\rm D}^{*+}\ell^-\overline{\nu}_\ell$ decays can be measured from the flight direction of the B meson and the energy of the missing neutrino. The large average decay length of the B meson (3 mm) and the precise vertex reconstruction ability provided by a silicon vertex detector can be used to measure the B meson direction by reconstructing its production and decay points. The granularity and the hermiticity of the ALEPH detector allow a measurement of the missing energy in a hemisphere due to the undetected neutrino.

This paper is organised as follows. After a brief description of the relevant components of the ALEPH detector in Section 2, the event selection is described in Section 3. The ω reconstruction procedure is described in Section 4. The relative abundances of weakly-decaying b hadrons in $\rm Z \to b\overline{b}$ decays are estimated in Section 5. Two important procedures developed to discriminate against non-exclusive $\overline{\rm B}^0 \to {\rm D}^{*+}\ell^-\overline{\nu}_\ell$ backgrounds are discussed in Section 6. Sections 7 and 8 describe the measurement of $\mathcal{F}(1)|V_{\rm cb}|$ and the systematic uncertainties.

2 The ALEPH Detector

The ALEPH detector is described in detail in Reference [10], and only a brief description of the apparatus is given here.

A high resolution vertex detector (VDET) consisting of two layers of double sided silicon microstrip detectors surrounds the beam pipe. The inner layer is at an average radius of 6.5 cm from the beam axis and covers 85% of the solid angle, while the outer layer is at an average radius of 11.3 cm and covers 69%. The spatial resolution for the $r\phi$ coordinate is 12 μm . The z coordinate resolution varies between 12 and 22 μm, depending on the polar angle of the track. The vertex detector is surrounded by a drift chamber (ITC) with eight axial wire layers up to a radius of 26 cm and a time projection chamber (TPC) that measures up to 21 three-dimensional points per track at radii between 30 and 180 cm. These detectors are immersed in an axial magnetic field of 1.5 T and together provide a momentum resolution of $\sigma_p/p = 0.0006p + 0.005$ (p in GeV/c). For tracks with hits in both layers of the VDET, the resolution of the impact parameter is $\sigma = 25\,\mu\mathrm{m} + 95\mu\mathrm{m}/p$ (p in GeV/c) in both the $r\phi$ and rz views. The TPC also provides up to 338 measurements of specific ionization of a charged particle. It is surrounded by an electromagnetic calorimeter (ECAL) of lead interleaved with proportional chambers, segmented into 15 mrad $\times$ 15 mrad projective towers and read out in three sections in depth, with energy resolution $\sigma_E/E = 0.18/\sqrt{E} + 0.009$ (E in GeV) for electromagnetic showers. The iron return yoke of the magnet is instrumented with streamer tubes to form a hadron calorimeter (HCAL), with a thickness of over 7 interaction lengths. It is surrounded by two additional double layers of streamer tubes for muon identification.

The analysis presented in this letter is based on approximately 3 million hadronic Z decays recorded from 1991 to 1994. The selection of hadronic events is based on charged particles and has been described elsewhere [11]. The interaction point is reconstructed on an event by event basis using the constraint of the average beam spot position [12, 13]. The resolution is 85μm, averaged over all directions for $\mathrm{b\overline{b}}$ events.

3 Event Selection

Candidates for the decay $\overline{\mathrm{B}}^0 \to \mathrm{D}^{*+}\ell^-\overline{\nu}_\ell$ are selected from events where a D^{*+} and a lepton are found in the same hemisphere with respect to the thrust axis of a hadronic Z decay. In this paper, "leptons" will refer to either electrons or muons, and charge conjugate reactions are always implied. Electrons are identified by comparing the momentum measured by the tracking detectors with the energy measured in the ECAL, by the depth and shape of the ECAL shower, and by the specific ionization information from the TPC when available. Muon candidates are accepted if they have a hit pattern characteristic of a penetrating particle in the HCAL and if they have at least one associated hit in the muon chambers. Electron and muon candidates must have momenta greater than 2 GeV/c and 3 GeV/c, respectively. Lepton identification in ALEPH is described in detail in Reference [10].

The D^{*+} candidates are reconstructed in the channel $\mathrm{D}^{*+} \to \mathrm{D}^0\pi^+$. The D^0 candidates are reconstructed in three decay modes: $\mathrm{D}^0 \to \mathrm{K}^-\pi^+$, $\mathrm{D}^0 \to \mathrm{K}^-\pi^+\pi^-\pi^+$, and $\mathrm{D}^0 \to \mathrm{K}^0_\mathrm{S}\pi^+\pi^-$. Candidate K^0_S are reconstructed via $\mathrm{K}^0_\mathrm{S} \to \pi^+\pi^-$.

The difference δ_m between the reconstructed masses of the $D^0\pi^+$ and the D^0 candidates must be within $2.1\,\mathrm{MeV}/c^2$ of $145.4\,\mathrm{MeV}/c^2$, which corresponds to approximately 2.5 times the average resolution for this quantity. The D^0 vertex must be separated from the interaction point by more than twice the resolution of the reconstructed decay distance for the candidate.

Charged kaon candidates for which dE/dx information is available must have a specific ionization within two standard deviations of the expected rate. In the $D^0 \to K^-\pi^+\pi^-\pi^+$ channel, kaon candidates with momenta less than $2\,\mathrm{GeV}/c$ are rejected. Candidate K^0_S must have a momentum larger than $0.5\,\mathrm{GeV}/c$, a decay length larger than 0.5 cm, and a reconstructed mass within $15\,\mathrm{MeV}/c^2$ of the nominal K^0_S mass.

Further criteria are applied so that selected events have topologically displaced vertices to allow measurement of the B meson direction. Vertex detector hits are required for the lepton candidate and at least two of the tracks originating from the D^0 candidate. The $D^{*+}\ell^-$ vertex is determined from the lepton and the D^0 candidates. The χ^2 probability of the vertex fit for each of the D^0 and $D^{*+}\ell^-$ vertices must be larger than 1%. To ensure a precise measurement of the B meson direction, $D^{*+}\ell^-$ candidates are rejected if the $D^{*+}\ell^-$ vertex is less than 1mm away from the interaction point. Finally, the reconstructed D^0 mass must lie within 2.5 standard deviations of the nominal value, where the average mass resolution is $10\,\mathrm{MeV}/c^2$ for $D^0 \to K^-\pi^+$ and $D^0 \to K^0_S\pi^+\pi^-$, and $8\,\mathrm{MeV}/c^2$ for $D^0 \to K^-\pi^+\pi^-\pi^+$. The selection results in a sample of 923 $D^{*+}\ell^-$ candidates.

4 ω Reconstruction

Equation 2 expresses ω in terms of the neutrino energy E_ν, and the angle ϕ between the planes formed by the D^{*+} and the lepton and by the B meson and the neutrino (Fig. 1):

$$\omega = 1/2m_{B^0}m_{D^{*+}} \times \Big\{m^2_{B^0} + m^2_{D^{*+}} - m^2_\ell - \Big[p_\ell \cos\theta_\ell (m^2_{B^0} - M^2)/P + 2E_\nu\,(E_\ell - p_\ell \cos\theta_\ell E/P) - 2p_\ell \sin\theta_\ell E_\nu \sin\theta_\nu \cos\phi\Big]\Big\}\,. \quad (2)$$

The variables M, P, and E are the mass, momentum, and energy of the reconstructed $D^{*+}\ell^-$.

The neutrino energy E_ν is estimated from the missing energy in the hemisphere containing the $D^{*+}\ell^-$ candidate, as described in reference [14]. The distribution of the difference between the reconstructed and the true neutrino energy has an rms of approximately 2.6 GeV in simulated $\overline{B}^0 \to D^{*+}\ell^-\overline{\nu}_\ell$ events. The variables θ_ℓ and θ_ν are, respectively, the opening angles of the lepton and the neutrino with respect to the axis defined by the $D^{*+}\ell^-$ system(Fig. 1). The angle θ_ν is calculated from E_ν:

$$\cos\theta_\nu = \frac{E}{P} - \frac{(m^2_{B^0} - M^2)}{2PE_\nu}\,. \quad (3)$$

In cases when the measurement of E_ν results in unphysical values for $\cos\theta_\nu$, E_ν is set to the corresponding physical limit defined by $\cos\theta_\nu = \pm 1$. The angle ϕ is calculated from the B meson direction as measured by the production and decay vertices.

Figure 2 shows a Monte Carlo simulation [15] of the reconstructed ω (denoted $\tilde{\omega}$) for events with measured decay lengths larger than 1mm. The average ω resolution is

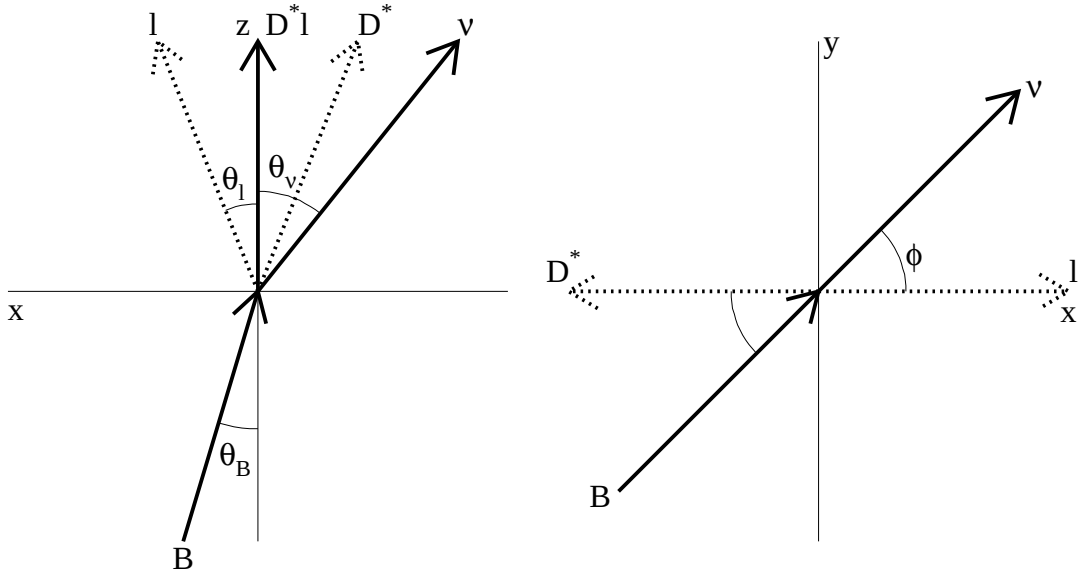

Figure 1: A schematic diagram showing the various lab-frame angles in a $\overline{\mathrm{B}}^0 \to \mathrm{D}^{*+}\ell^-\overline{\nu}_\ell$ decay. The coordinate system is chosen so the $\mathrm{D}^{*+}\ell^-$ defines the z-axis, and the perpendicular to the plane containing the D^{*+} and the lepton defines the y-axis.

approximately 0.07, which corresponds to about 14% of the allowed range. The resolution is dominated by the measurement uncertainty in ϕ.

The opening angle θ_B between the reconstructed B meson direction and the $\mathrm{D}^{*+}\ell^-$ direction can be used in conjunction with the measured neutrino energy to construct a variable M^2_{miss} which is sensitive to the presence of additional particles coming from the B meson decay vertex:

$$M^2_{\mathrm{miss}} = m^2_{\mathrm{B}^0} + M^2 - 2\,(E + E_\nu)\left(E - \sqrt{1 - m^2_{\mathrm{B}^0}/(E+E_\nu)^2}\,P\cos\theta_\mathrm{B}\right) . \qquad (4)$$

5 Estimate of b Hadron Fractions

The fraction of B^0 mesons produced in $\mathrm{Z} \to \mathrm{b\overline{b}}$ decays is needed for the measurement of the partial width. The fractions of other weakly-decaying b hadron species produced in $\mathrm{Z} \to \mathrm{b\overline{b}}$ decays are also required to determine the $\mathrm{D}^{*+}\ell^-$ sample composition. The fractions of B^0_s and b baryons produced are estimated from measured branching fraction products from $\mathrm{D}^+_\mathrm{s}\ell^-$ and $\Lambda^+_\mathrm{c}\ell^-$ correlations, and are used to infer the fractions of B^0 and B^- mesons in $\mathrm{Z} \to \mathrm{b\overline{b}}$ decays.

The fraction, $f_{\mathrm{B}^0_\mathrm{s}}$, of B^0_s mesons produced is estimated from the product branching fraction $f_{\mathrm{B}^0_\mathrm{s}} \cdot \mathrm{Br}(\overline{\mathrm{B}}^0_\mathrm{s} \to \mathrm{D}^+_\mathrm{s} X\ell^-\overline{\nu}_\ell) = 0.92 \pm 0.09 \pm 0.16\%$, measured using $\mathrm{D}^+_\mathrm{s}\ell^-$ correlations [16]. The quantity $\mathrm{Br}(\overline{\mathrm{B}}^0_\mathrm{s} \to \mathrm{D}^+_\mathrm{s} X\ell^-\overline{\nu}_\ell)$ is estimated from the product of the B^0_s semileptonic branching fraction $\mathrm{Br}(\overline{\mathrm{B}}^0_\mathrm{s} \to X\ell^-\overline{\nu}_\ell)$ and the fraction $f^{\mathrm{sl}}_{\mathrm{D}^+_\mathrm{s}}$ of these decays producing a D^+_s.

The value of $\mathrm{Br}(\overline{\mathrm{B}}^0_\mathrm{s} \to X\ell^-\overline{\nu}_\ell)$ is estimated from the semileptonic branching fractions

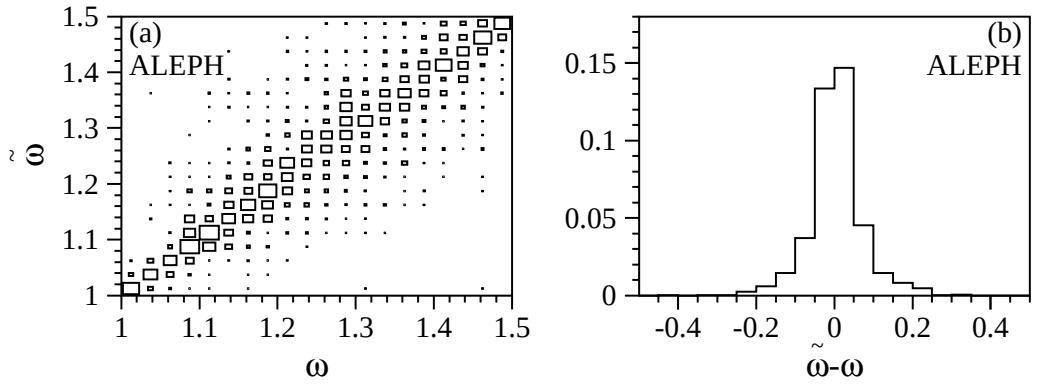

Figure 2: Monte Carlo simulation of the ω reconstruction for $\overline{\mathrm{B}}^0 \to \mathrm{D}^{*+}\ell^-\overline{\nu}_\ell$ events. (a) The reconstructed ω (denoted $\tilde{\omega}$) as a function of the input ω. The area of each box is proportional to the number of events. (b) The ω resolution $\tilde{\omega} - \omega$ averaged over all ω.

of other b hadrons assuming equality of semileptonic partial widths. The partial width $\Gamma^{\mathrm{sl}} \equiv \Gamma(\mathrm{b} \to X\ell^-\overline{\nu}_\ell)$ is obtained from $\mathrm{Br}(\overline{\mathrm{B}} \to X\ell^-\overline{\nu}_\ell)$ measured at the $\Upsilon(4\mathrm{S})$ resonance and the corresponding B^0 and B^+ lifetimes, and from $\mathrm{Br}(\mathrm{b} \to X\ell^-\overline{\nu}_\ell)$ measured at the Z resonance using the average b hadron lifetime (Tables 1 and 2). The results are $\Gamma^{\mathrm{sl}}_{\Upsilon(4\mathrm{S})} = (6.37 \pm 0.24) \times 10^{-2}\mathrm{ps}^{-1}$ and $\Gamma^{\mathrm{sl}}_{\mathrm{Z}} = (7.15 \pm 0.19) \times 10^{-2}\mathrm{ps}^{-1}$. To account for this apparent discrepancy, the value $\Gamma^{\mathrm{sl}} = (6.76 \pm 0.39) \times 10^{-2}\mathrm{ps}^{-1}$ is used, which is the arithmetic mean with an uncertainty spanning the difference. Using the measured B^0_s lifetime, the branching fraction is then $\mathrm{Br}(\overline{\mathrm{B}}^0_\mathrm{s} \to X\ell^-\overline{\nu}_\ell) = 10.5 \pm 1.0\%$.

The fraction $f^{\mathrm{sl}}_{\mathrm{D}^+_\mathrm{s}}$ is calculated from the branching fractions for the decays $\overline{\mathrm{B}} \to \mathrm{D}\ell^-\overline{\nu}_\ell$ [17], $\overline{\mathrm{B}} \to \mathrm{D}^*\ell^-\overline{\nu}_\ell$ [9, 17], and $\mathrm{B}^- \to \mathrm{D}^{*+}\pi^-\ell^-\overline{\nu}_\ell$ [18], using symmetries and the equality of partial widths. In the $\mathrm{B}^0/\mathrm{B}^-$ system, decays to $\mathrm{D}\ell^-\overline{\nu}_\ell$ and $\mathrm{D}^*\ell^-\overline{\nu}_\ell$ account for $62 \pm 5\%$ of the semileptonic decay rate. The corresponding modes in the B^0_s system, $\overline{\mathrm{B}}^0_\mathrm{s} \to \mathrm{D}^+_\mathrm{s}\ell^-\overline{\nu}_\ell$ and $\overline{\mathrm{B}}^0_\mathrm{s} \to \mathrm{D}^{*+}_\mathrm{s}\ell^-\overline{\nu}_\ell$, are assumed to account for 62% of $\overline{\mathrm{B}}^0_\mathrm{s} \to X\ell^-\overline{\nu}_\ell$. An upper bound can be derived from the branching fraction for $\mathrm{B}^- \to \mathrm{D}^{*+}\pi^-\ell^-\overline{\nu}_\ell$, as the equivalent decay in the B^0_s system, $\overline{\mathrm{B}}^0_\mathrm{s} \to \mathrm{D}^{*+}\mathrm{K}^0\ell^-\overline{\nu}_\ell$, does not enter the $\mathrm{D}^+_\mathrm{s}\ell^-$ sample:

$$\Gamma(\mathrm{B}^- \to \mathrm{D}^{*+}\pi^-\ell^-\overline{\nu}_\ell) = \Gamma(\overline{\mathrm{B}}^0_\mathrm{s} \to \mathrm{D}^{*+}\mathrm{K}^0\ell^-\overline{\nu}_\ell) = \Gamma(\overline{\mathrm{B}}^0_\mathrm{s} \to \mathrm{D}^{*0}\mathrm{K}^+\ell^-\overline{\nu}_\ell)\,,$$

assuming SU(3) flavour symmetry in the first equality and isospin symmetry in the second. The result is $\mathrm{Br}(\overline{\mathrm{B}}^0_\mathrm{s} \to (\mathrm{D}^*\mathrm{K})\ell^-\overline{\nu}_\ell) = 2.0 \pm 0.7\%$, corresponding to an upper bound for $f^{\mathrm{sl}}_{\mathrm{D}^+_\mathrm{s}}$ of 81%. In accordance with the lower and upper bounds, the fraction of semileptonic B^0_s decays containing D^+_s is taken to be $f^{\mathrm{sl}}_{\mathrm{D}^+_\mathrm{s}} = 72 \pm 10\%$.

Combining the above results, the estimated fraction of b quarks that hadronise to B^0_s mesons is

$$f_{\mathrm{B}^0_\mathrm{s}} = 12.2 \pm 1.2_{\mathrm{stat}} \pm 2.9_{\mathrm{syst}}\% \,.$$

An analogous procedure is followed to estimate f_{Λ_b}, the fraction of weakly-decaying b baryons. Using $\Lambda^+_\mathrm{c}\ell^-$ correlations, the measured branching fraction product $f_{\Lambda_\mathrm{b}} \cdot$

Channel	Branching Fraction(%)	Reference
$\Gamma(Z \to b\overline{b})/\Gamma(Z \to \text{hadrons})$	22.02 ± 0.20	[20]
$b \to X\ell^-\overline{\nu}_\ell$	10.99 ± 0.25	[20]
$\overline{B} \to X\ell^-\overline{\nu}_\ell$	10.29 ± 0.28	[21]
$\overline{B} \to D\ell^-\overline{\nu}_\ell$	1.80 ± 0.41	[17]
$\overline{B} \to D^*\ell^-\overline{\nu}_\ell$	4.56 ± 0.29	[9, 17]
$b \to D^{*+}\pi^-\ell^-\overline{\nu}_\ell X$	0.37 ± 0.12	[18]
$\overline{B}^0 \to D^{*+}\tau^-\overline{\nu}_\tau$	2.1 ± 0.4	-
$\overline{B} \to D^{*+}X_c$	5.2 ± 1.7	-

Table 1: Branching fractions used in calculating the fractions of b hadrons in $Z \to b\overline{b}$ decay and in the estimation of the background in the $D^{*+}\ell^-$ sample. The unreferenced entries are estimated in Section 6.

Species	Lifetime (ps)
B^0	1.58 ± 0.06
B^-	1.65 ± 0.06
B_s^0	1.55 ± 0.11
Λ_b^0	1.20 ± 0.08
Average b	1.538 ± 0.022

Table 2: Lifetimes used in this paper. All lifetimes are taken from [22].

$\mathrm{Br}(\Lambda_b^0 \to \Lambda_c^+ X\ell^-\overline{\nu}_\ell)$ is $0.76 \pm 0.15 \pm 0.12\%$ [19]. Using the measured b baryon lifetime (Table 2) and proceeding as above, the b baryon semileptonic branching fraction is estimated to be $\mathrm{Br}(\Lambda_b^0 \to X\ell^-\overline{\nu}_\ell) = 8.1 \pm 0.7\%$. The estimated fraction of such decays that contain a Λ_c^+ is $f^{\mathrm{sl}}_{\Lambda_c^+} = 81 \pm 19\,\%$, where the lower bound is determined as above but the upper bound is taken to be 100%. The fraction of b quarks that hadronise to b baryons is then

$$f_{\Lambda_b} = 11.5 \pm 2.2_{\mathrm{stat}} \pm 3.4_{\mathrm{syst}}\% \,.$$

The fractions f_{B^0} and f_{B^+} are derived from the above results assuming $f_{B^0} + f_{B^+} + f_{B_s^0} + f_{\Lambda_b} = 1$ and $f_{B^0} = f_{B^+}$, with the result

$$f_{B^0} = f_{B^+} = 38.2 \pm 1.3_{\mathrm{stat}} \pm 2.2_{\mathrm{syst}}\% \,.$$

6 Sample Composition and Background Rejection

Table 3 shows the expected composition of the initial selected sample of $D^{*+}\ell^-$ events. The rates for some of the contributing processes have not been measured and are estimated from other measurements. Isospin and flavour SU(3) symmetry are used to relate the branching fractions for the processes $\overline{B}^0 \to D^{*+}\pi^0\ell^-\overline{\nu}_\ell$ and $\overline{B}_s^0 \to D^{*+}K^0\ell^-\overline{\nu}_\ell$ to the recent ALEPH measurement of $\mathrm{Br}(B^- \to D^{*+}\pi^-\ell^-\overline{\nu}_\ell)$ [18]. The branching fraction

	Initial	Final
Yield	923 ± 30.4	570 ± 23.8
Background		
Combinatorial	203.6 ± 12.2	86.2 ± 7.2
$\mathrm{B}^- \to \mathrm{D}^{*+}\pi^-\ell^-\overline{\nu}_\ell$	110.3 ± 35.8	17.1 ± 5.5
$\overline{\mathrm{B}} \to \mathrm{D}^{*+}\pi^0/\mathrm{K}^0\ell^-\overline{\nu}_\ell$	90.3 ± 29.3	44.8 ± 14.5
$\overline{\mathrm{B}}^0 \to \mathrm{D}^{*+}\tau^-\overline{\nu}_\tau$	29.5 ± 5.6	5.2 ± 1.0
$\overline{\mathrm{B}} \to \mathrm{D}^{*+}X_\mathrm{c}$	19.8 ± 6.5	6.4 ± 2.1
Total Background	453.5 ± 66.8	159.7 ± 21.4
Signal	469.5 ± 73.4	410.3 ± 32.0

Table 3: The $\mathrm{D}^{*+}\ell^-$ yield and the estimated background for the initial sample and after applying the background rejection criteria.

$\mathrm{Br}(\overline{\mathrm{B}}^0 \to \mathrm{D}^{*+}\tau^-\overline{\nu}_\tau)$ is calculated from the ALEPH measurement of inclusive τ production in b decays [23] and the assumption that three-fourths of B^0 decays to τ leptons involve D^{*+}, consistent with spin counting arguments. The inclusive branching fraction for the production of a D^{*+} meson in association with another charm hadron is estimated from measured branching fraction for $\overline{\mathrm{B}}^0 \to \mathrm{D}^{*+}\mathrm{D}_\mathrm{s}^{(*)-}$ [17] scaled by 1.2 ± 0.2 to allow for the possibility of n-body($n \geq 3$) decays.

The production fractions for weakly-decaying b hadrons are estimated in Section 5. The fraction of hadronic Z decays to $\mathrm{b\overline{b}}$ pairs is taken from [20]. All other branching fractions are taken from [17].

Three classes of combinatorial background are present in the sample. One class of background arises from random combinations of tracks lying within the D^0 and δ_m mass windows. This is estimated from fits to the D^0 mass peaks using a Gaussian for the signal and a first order polynomial for the combinatorial background. The background estimate is calculated from the integral of the fitted background function over the D^0 mass window. The second class of combinatorial background is from true D^0 candidates combined with a random slow pion giving a reconstructed mass difference within the δ_m mass window. This is estimated from the scaled D^0 yield in the δ_m sideband. The final class of combinatorial background is from true D^{*+} mesons associated with misidentified hadrons or non-prompt leptons. Background from misidentified hadrons is estimated by applying the measured misidentification rate [10] to D^{*+}-hadron combinations selected in the data. Additional background from non-prompt leptons is estimated from the simulation.

The contribution of the background process $\overline{\mathrm{B}} \to \mathrm{D}^{*+}\pi/\mathrm{K}\,\ell^-\overline{\nu}_\ell$ is large and is not precisely known and dominates the uncertainty in the signal yield. To reduce this background, two additional event selection criteria are used. One method of background suppression is topological. In candidate events, tracks having momenta greater than $0.5\,\mathrm{GeV}/c$, at least one VDET hit, and the same charge as the lepton candidate are selected. The signed impact parameter of these tracks with respect to the $\mathrm{D}^{*+}\ell^-$ vertex is calculated (the sign is negative if the track's point of closest approach to the vertex is upstream from the reconstructed $\mathrm{D}^{*+}\ell^-$ vertex). Tracks from the interaction point tend to have negative impact parameters, while tracks originating from the $\mathrm{D}^{*+}\ell^-$ vertex are distributed symmetrically

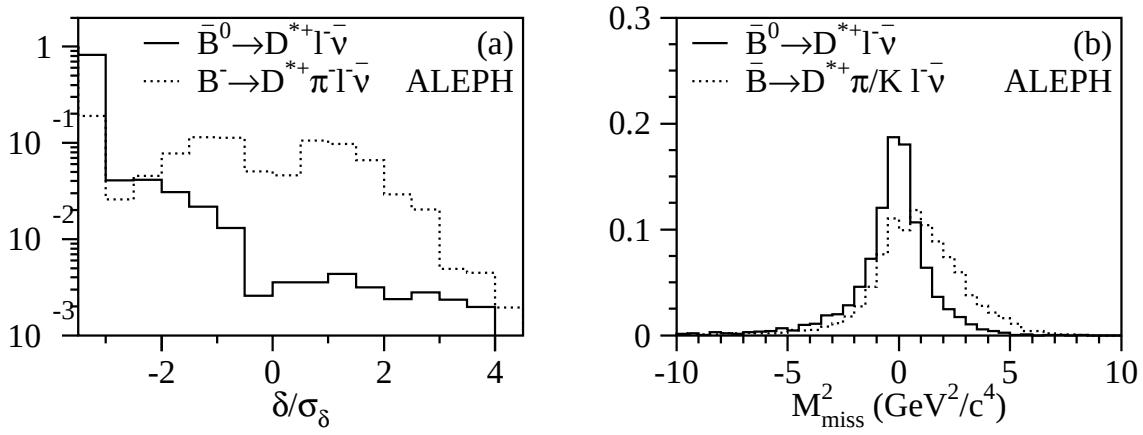

Figure 3: Two methods of background rejection. (a)The impact parameter significance of tracks with respect to the $D^{*+}\ell^-$ vertex for simulated $\overline{B}^0 \to D^{*+}\ell^-\overline{\nu}_\ell$ and $B^- \to D^{*+}\pi^-\ell^-\overline{\nu}_\ell$ events with reconstructed decay lengths larger than 1 mm. The leftmost bin includes candidates where no tracks were found with impact parameter significance larger than -3. The vertical scale is logarithmic and the histograms are normalized to unit area. (b)The reconstructed $M^2_{\rm miss}$ for simulated $\overline{B}^0 \to D^{*+}\ell^-\overline{\nu}_\ell$ events and $\overline{B} \to D^{*+}\pi/K\,\ell^-\overline{\nu}_\ell$ events. The histograms are normalized to unit area.

about zero. Candidates accompanied by one or more selected tracks with impact parameters between -2 and 3 times the calculated error are rejected. This requirement is designed to remove $B^- \to D^{*+}\pi^-\ell^-\overline{\nu}_\ell$ events. From Monte Carlo simulation, this requirement has an efficiency of 92% for signal events and rejects 70% of the $B^- \to D^{*+}\pi^-\ell^-\overline{\nu}_\ell$ background. Figure 3a shows the distribution of the signed impact parameter for simulated signal and $B^- \to D^{*+}\pi^-\ell^-\overline{\nu}_\ell$ events.

To suppress background events with additional particles originating from the b hadron decay, a requirement is placed on the calculated $M^2_{\rm miss}$; candidates with a reconstructed $M^2_{\rm miss}$ larger than $1\,{\rm GeV}^2/c^4$ are rejected. In contrast to the topological requirement, this is also effective in removing events with additional neutral particles originating at the decay vertex. Figure 3b shows the missing mass-squared spectrum for simulated $\overline{B} \to D^{*+}\pi/K\,\ell^-\overline{\nu}_\ell$ events. In the Monte Carlo simulation this requirement has an efficiency of 83% for signal events, and rejects 45% of the $\overline{B} \to D^{*+}\pi/K\,\ell^-\overline{\nu}_\ell$ background.

Imposing these two criteria results in a sample of 570 $D^{*+}\ell^-$ candidates. Table 4 shows the number of candidates and the estimated combinatorial background in each channel. Table 3 summarizes the yields and the estimated background. The contribution of all background sources has been drastically reduced. In particular, $\overline{B} \to D^{*+}\pi/K\,\ell^-\overline{\nu}_\ell$ is estimated to be approximately 10% of the sample.

Mode	$K^-\pi^+$	$K^-\pi^+\pi^-\pi^+$	$K^0_S\pi^+\pi^-$	Total
Raw Yield	226 ± 15.0	273 ± 16.5	71 ± 8.4	570 ± 23.8
Combinatorial Background				
Fake D^0	12.2 ± 2.1	32.3 ± 2.9	4.1 ± 1.2	48.6 ± 3.8
Fake D^{*+}	9.6 ± 3.2	5.8 ± 4.3	3.4 ± 2.2	18.8 ± 5.8
Fake ℓ	8.1 ± 0.8	8.7 ± 0.9	2.0 ± 0.2	18.8 ± 1.9
Total	29.9 ± 3.9	46.8 ± 5.3	9.5 ± 2.5	86.2 ± 7.2
Net Yield	196.1 ± 15.5	226.2 ± 17.3	61.5 ± 8.8	483.8 ± 24.9

Table 4: The $D^{*+}\ell^-$ yield and the estimated combinatorial background after background suppression.

7 Measurement of $\mathcal{F}(1)|V_{cb}|$

A unbinned maximum likelihood fit is performed to the reconstructed ω spectrum. The fitting function is given in Eq. 1, with the following assumed functional form for $\mathcal{F}(\omega)$:

$$\mathcal{F}(\omega) = \mathcal{F}(1)\left[1 + a^2(1-\omega)\right] . \tag{5}$$

The two free parameters in the fit are $\mathcal{F}(1)|V_{cb}|$ and a^2. The fitting function is convolved with a resolution function and a ω-dependent efficiency.

A numerical resolution function is determined from a Monte Carlo simulation. The efficiency is also estimated from the Monte Carlo simulation, but corrections are applied based on detailed comparisons with the data. The efficiency of a given selection requirement is measured separately in the data and the Monte Carlo, and a correction factor is calculated from the ratio of the efficiencies. The simulated efficiency is then scaled by these correction factors. The simulated lepton identification efficiency is scaled by 0.97 ± 0.03 based on studies in [10]. The efficiencies for D^{*+} selection and the topological requirements are investigated using inclusive D^{*+} and $D^0\ell^-$ samples that are largely statistically independent from the sample considered here. Figure 4 shows the corrected efficiency for each channel as a function of ω.

The fit yields the following results, which are 91% correlated:

$$\begin{aligned} \mathcal{F}(1)|V_{cb}| &= (31.4 \pm 2.3) \times 10^{-3} , \\ a^2 &= 0.39 \pm 0.21 , \end{aligned}$$

where the errors are statistical only. The fit is shown in Fig. 5a and Fig. 5b shows a graph of the product $|V_{cb}|\mathcal{F}(\omega)$ as a function of $\tilde{\omega}$.

While the data are consistent with a linear form for $\mathcal{F}(\omega)$, there is no theoretical justification ruling out other parametrisations [24]. A fit is performed using a second order polynomial of the form $\mathcal{F}(\omega) = \mathcal{F}(1)\left[1 + a^2(1-\omega) + b(1-\omega)^2\right]$, yielding the following results:

$$\begin{aligned} \mathcal{F}(1)|V_{cb}| &= (30.4 \pm 3.6) \times 10^{-3} , \\ a^2 &= 0.10 \pm 1.00 , \\ b &= -0.57 \pm 1.97 , \end{aligned}$$

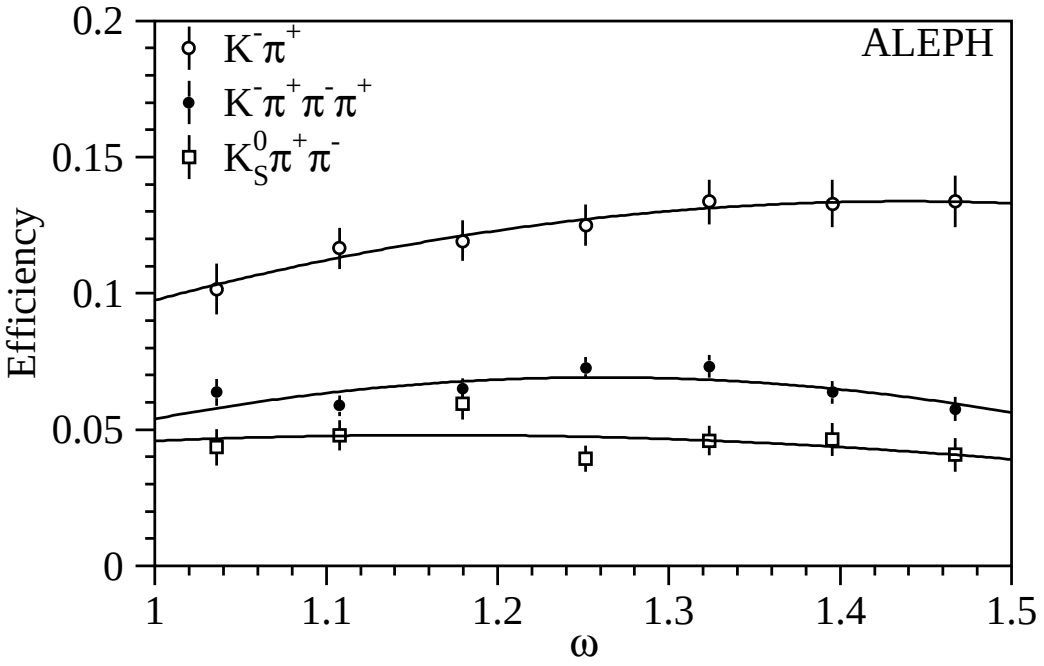

Figure 4: The corrected efficiency as a function of ω estimated from a Monte Carlo simulation of $\overline{\mathrm{B}}^0 \to \mathrm{D}^{*+}\ell^-\overline{\nu}_\ell$. The curves are parabolic parametrisations of the efficiency for each channel.

where the errors are statistical only. The result for $\mathcal{F}(1)|V_{\mathrm{cb}}|$ is consistent with that of the linear fit, though the uncertainty is increased due to the additional degree of freedom.

With the present data sample it is not possible to distinguish between the linear parametrisation and parametrisations with more degrees of freedom. Consequently, the results in this paper are obtained with the linear parametrisation.

The same data sample is also used to extract a measurement of $\mathrm{Br}(\overline{\mathrm{B}}^0 \to \mathrm{D}^{*+}\ell^-\overline{\nu}_\ell)$:

$$\mathrm{Br}(\overline{\mathrm{B}}^0 \to \mathrm{D}^{*+}\ell^-\overline{\nu}_\ell) = (5.18 \pm 0.30)\% \,,$$

where the quoted error is statistical only.

8 Systematic Uncertainties

Various sources of systematic uncertainties have been considered. Their respective contribution are summarized in Table 5.

Branching Fractions: The systematic uncertainties related to the fraction of Z decays to $\mathrm{b\overline{b}}$ pairs, f_{B^0} and the D^{*+} and D^0 branching fractions were estimated by the effect of a variation by the quoted errors, including correlations in the measured branching fractions. The dominant systematic uncertainty is from f_{B^0}. The total systematic uncertainty from these sources is 4.3% on $\mathcal{F}(1)|V_{\mathrm{cb}}|$ and 8.6% on $\mathrm{Br}(\overline{\mathrm{B}}^0 \to \mathrm{D}^{*+}\ell^-\overline{\nu}_\ell)$.

Physics Background: The contribution of each physics background process to the final $\mathrm{D}^{*+}\ell^-$ sample was varied within the uncertainties quoted in Table 1. As the contributions of events from the processes $\overline{\mathrm{B}} \to \mathrm{D}^{*+}\pi/\mathrm{K}\,\ell^-\overline{\nu}_\ell$ are proportional to a single

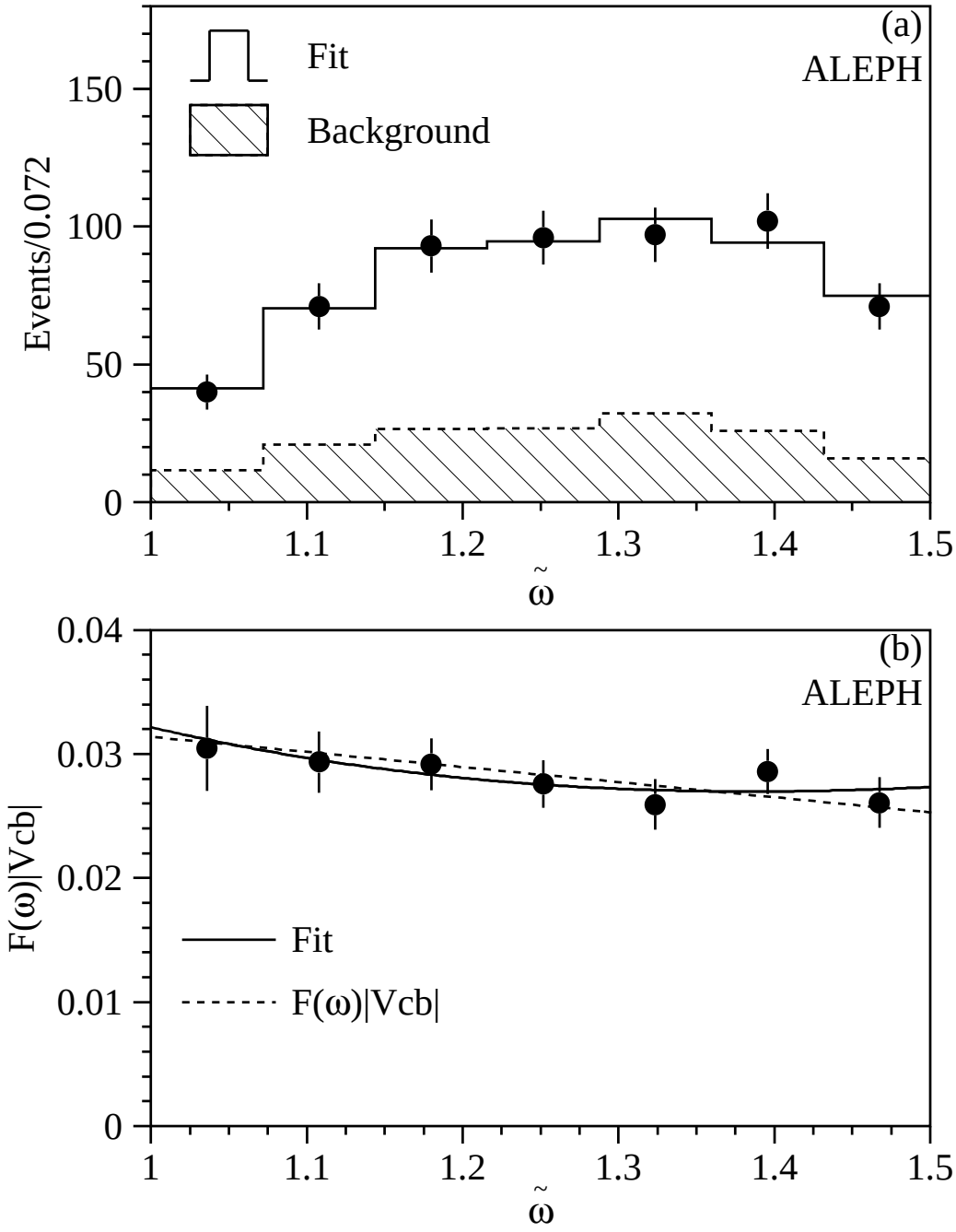

Figure 5: (a)The differential yield $dN/d\tilde{\omega}$. The points are the data, the histogram shows the result of fit and the hatched area is the estimated background. (b)The product $|V_{\rm cb}|\mathcal{F}(\omega)$ as a function of $\tilde{\omega}$. The points are background-subtracted data for the square root of the measured decay rate divided by factors other than $\mathcal{F}(\omega)|V_{\rm cb}|$ in Eq. 1. The solid curve is the fit. The dashed curve shows the underlying distribution before convolution with the resolution function. The value of $\mathcal{F}(1)|V_{\rm cb}|$ corresponds to the intercept of this curve. The difference between the two curves shows the effect of the resolution.

Source	ΔBr/Br (%)	$\Delta\lvert V_{cb}\rvert/\lvert V_{cb}\rvert$ (%)	Δa^2
Branching Fractions			
f_{B^0}	6.5	3.2	-
$D^{*+} \to D^0\pi^+$	2.8	1.5	-
$D^0 \to K^-\pi^+, K^-\pi^+\pi^-\pi^+, K^0_S\pi^+\pi^-$	4.7	2.4	-
$\Gamma(Z \to b\overline{b})/\Gamma(Z \to \text{hadrons})$	1.0	0.5	-
Subtotal	8.6	4.3	-
Physics Background			
$\overline{B} \to D^{*+}\pi/K\,\ell^-\overline{\nu}_\ell$	4.5	3.5	0.03
$\overline{B} \to D^{*+}X_c$	0.7	-	-
$\overline{B}^0 \to D^{*+}\tau^-\overline{\nu}_\tau$	0.3	0.1	-
Subtotal	4.6	3.5	0.03
Combinatorial Background			
Fake D^0	0.9	0.6	0.01
Fake D^{*+}	2.0	1.4	0.01
Fake lepton	0.8	0.4	0.01
Subtotal	2.3	1.6	0.02
Simulation			
MC statistics	1.6	1.7	0.05
Fragmentation	2.9	1.6	-
Efficiency	5.6	2.8	-
Subtotal	6.5	3.6	0.05
τ_{B^0}	1.7	2.6	-
Fitting Method	-	3.0	0.10
Total	12.0	7.9	0.12

Table 5: Summary of systematic uncertainties. Entries with a negligible uncertainty are left blank.

measurement [18], the corresponding errors have been added linearly. In accordance with the quoted measurement, the fraction of narrow-resonant decays in the Monte Carlo simulation was taken to be 55% and was varied from 0 to 100% to account for the lack of knowledge of $\overline{\mathrm{B}} \to \mathrm{D}^{*+}\pi/\mathrm{K}\,\ell^-\overline{\nu}_\ell$ decays. The total systematic uncertainty from physics background processes is 3.5% on $\mathcal{F}(1)|V_{\mathrm{cb}}|$ and 4.6% on $\mathrm{Br}(\overline{\mathrm{B}}^0 \to \mathrm{D}^{*+}\ell^-\overline{\nu}_\ell)$.

Combinatorial Background: The combinatorial background consists of three different sources: fake D^0, fake D^{*+}, and fake leptons. The first two are estimated from sidebands and the error is taken from the statistical precision. The error from the third source is due to the uncertainty in the simulation of non-prompt leptons. The total systematic uncertainty from the combinatorial background is 1.6% on $\mathcal{F}(1)|V_{\mathrm{cb}}|$ and 2.3% on $\mathrm{Br}(\overline{\mathrm{B}}^0 \to \mathrm{D}^{*+}\ell^-\overline{\nu}_\ell)$.

Simulation: The finite Monte Carlo sample size primarily affects the knowledge of the shape of the efficiency curves. The size of the background Monte Carlo sample is also taken into account.

The mean fraction of the beam energy taken by the B meson has been measured by ALEPH to be 0.714 ± 0.012 [25]. The precision of this measurement translates into an uncertainty on the reconstruction efficiency due to the dependence of the efficiency on the B^0 momentum. The systematic error due to this uncertainty is 1.6% for $\mathcal{F}(1)|V_{\mathrm{cb}}|$ and 2.9% for $\mathrm{Br}(\overline{\mathrm{B}}^0 \to \mathrm{D}^{*+}\ell^-\overline{\nu}_\ell)$.

The reconstruction efficiencies for both signal and physics background processes were estimated from Monte Carlo simulation. Comparisons of the efficiency for various selection criteria in data and the simulation result in an overall systematic uncertainty of 2.8% on $\mathcal{F}(1)|V_{\mathrm{cb}}|$ and 5.6% on $\mathrm{Br}(\overline{\mathrm{B}}^0 \to \mathrm{D}^{*+}\ell^-\overline{\nu}_\ell)$. The results are insensitive to the precise description of the form factors in the simulated $\overline{\mathrm{B}}^0 \to \mathrm{D}^{*+}\ell^-\overline{\nu}_\ell$ decays.

B^0 Lifetime: A change in the B^0 lifetime affects $\mathcal{F}(1)|V_{\mathrm{cb}}|$ in two ways. From Eq. 1, an increase in the lifetime will decrease the partial width for the same measured branching fraction. The branching fraction will also decrease because the 1 mm requirement on the decay length and the physics background rejection favour events with longer proper decay times. From the lifetime values quoted in Table 2, the calculated uncertainty is 2.6% on $\mathcal{F}(1)|V_{\mathrm{cb}}|$ and 1.7% on $\mathrm{Br}(\overline{\mathrm{B}}^0 \to \mathrm{D}^{*+}\ell^-\overline{\nu}_\ell)$. The uncertainty in the B^- and $\mathrm{B}_{\mathrm{s}}^0$ lifetimes also affects the proportion of physics background but the effect is negligible.

Fitting Method: The results are insensitive to the knowledge of the resolution function. If resolution effects are ignored while performing the fit, the resulting change in $\mathcal{F}(1)|V_{\mathrm{cb}}|$ is 2.4%. Moreover, if the resolution function is calculated after introducing a systematic 2 GeV shift in the reconstructed neutrino energy in the simulation (which is much larger than the absolute calibration error of the visible energy), the fit results for $\mathcal{F}(1)|V_{\mathrm{cb}}|$ are changed by a negligible amount. The effect on the calculated resolution function from the application of additional smearing to the reconstructed vertices in the simulation also has a negligible effect on the fit result. Using a linear parametrisation of the efficiency as a function of ω changes the fitted result for $\mathcal{F}(1)|V_{\mathrm{cb}}|$ by 0.5 %.

From studies of the stability of the results with respect to details of the fitting procedure, and from the studies mentioned above, an overall error of 0.10 is assigned to the value of a^2, translating into an uncertainty of 3% on $\mathcal{F}(1)|V_{\mathrm{cb}}|$.

Including the systematic uncertainties, the following values are obtained for $\mathcal{F}(1)|V_{\mathrm{cb}}|$

and a^2:

$$\begin{aligned} \mathcal{F}(1)|V_{\rm cb}| &= (31.4 \pm 2.3_{\rm stat} \pm 2.5_{\rm syst}) \times 10^{-3} , \\ a^2 &= 0.39 \pm 0.21_{\rm stat} \pm 0.12_{\rm syst} . \end{aligned}$$

The result for the branching fraction is

$$\mathrm{Br}(\overline{\mathrm{B}}^0 \to \mathrm{D}^{*+}\ell^-\overline{\nu}_\ell) = (5.18 \pm 0.30_{\rm stat} \pm 0.62_{\rm syst})\% .$$

9 Conclusion

The differential rate $d\Gamma/d\omega$ for the decay $\overline{\mathrm{B}}^0 \to \mathrm{D}^{*+}\ell^-\overline{\nu}_\ell$ is measured, and a value for $\mathcal{F}(1)|V_{\rm cb}|$ is extracted from a fit:

$$\begin{aligned} \mathcal{F}(1)|V_{\rm cb}| &= (31.4 \pm 2.3_{\rm stat} \pm 2.5_{\rm syst}) \times 10^{-3} , \\ a^2 &= 0.39 \pm 0.21_{\rm stat} \pm 0.12_{\rm syst} . \end{aligned}$$

These results are consistent with the most precise previous measurement to date [9], and are of comparable precision. The result for a^2 is also consistent with theoretical bounds [7].

Taking $\mathcal{F}(1) = 0.91 \pm 0.04$ [7], the result for $|V_{\rm cb}|$ is

$$|V_{\rm cb}| = (34.5 \pm 2.5_{\rm stat} \pm 2.7_{\rm syst} \pm 1.5_{\rm theory}) \times 10^{-3} ,$$

where the third error is from the quoted theoretical uncertainty in the calculation of $\mathcal{F}(1)$.

From the integrated spectrum, the measured branching fraction is

$$\mathrm{Br}(\overline{\mathrm{B}}^0 \to \mathrm{D}^{*+}\ell^-\overline{\nu}_\ell) = (5.18 \pm 0.30_{\rm stat} \pm 0.62_{\rm syst})\% .$$

These results are based on the best available knowledge of f_{B^0} and τ_{B^0}. To a good approximation, results corresponding to different values of f_{B^0} and τ_{B^0} can be calculated using Table 5:

$$\begin{aligned} \mathcal{F}(1)|V_{\rm cb}| &= [31.4 - 0.4(f_{\mathrm{B}^0} - 38.2) - 14(\tau_{\mathrm{B}^0} - 1.58)] \times 10^{-3} \\ \mathrm{Br}(\overline{\mathrm{B}}^0 \to \mathrm{D}^{*+}\ell^-\overline{\nu}_\ell) &= [5.18 - 0.13(f_{\mathrm{B}^0} - 38.2) - 1.5(\tau_{\mathrm{B}^0} - 1.58)]\% , \end{aligned}$$

with lifetimes in ps, and branching fractions in percent.

Acknowledgements

We are indebted to our colleagues in the accelerator divisions for the excellent performance of the LEP storage ring. We also thank the engineers and technicians of the collaborating institutions for their support in constructing the ALEPH experiment. Those of us from non-member states thank CERN for its hospitality.

References

[1] N. Isgur and M. Wise, Phys. Lett. B **232** (1989) 113, Phys. Lett. B **237** (1990) 527.

[2] H. Georgi, Phys. Lett. B **240** (1990) 447.

[3] E. Eichten and B. Hill, Phys. Lett. B **234** (1990) 511.

[4] M. Neubert, Phys. Lett. B **264** (1991) 455.

[5] M. Shifman, N.G. Uraltsev and A. Vainshtein, Phys .Rev. D **51** (1995) 2217.
I. Bigi, M. Shifman, N.G. Uraltsev, and A. Vainshtein, preprint TPI-MINN-94/12-T (1994).

[6] M. Neubert, Phys. Lett. B **338**, (1994) 84.

[7] M. Neubert, preprint CERN-TH/95-107, (1995).

[8] H. Albrecht *et al.* (ARGUS Collab.), Phys. Lett. B **197** (1987) 452.
D. Borteletto *et al.* (CLEO Collab.), Phys. Rev. Lett. **63** (1989) 1667.
R. Fulton *et al.* (CLEO Collab.), Phys. Rev. D **43** (1991) 651.
H. Albrecht *et al.* (ARGUS Collab.), Phys. Lett. B **275** (1992) 195.
H. Albrecht *et al.* (ARGUS Collab.), Phys. Lett. B **324** (1994) 249.
H. Albrecht *et al.* (ARGUS Collab.), Z. Phys. C **57** (1993) 533.

[9] B. Barish *et al.* (CLEO Collab.), Phys. Rev. D **51** (1995) 1014.

[10] D. Decamp *et al.* (ALEPH Collab.), Nucl. Instrum. Methods A **294** (1990) 121.
D. Buskulic *et al.* (ALEPH Collab.), Nucl. Instrum. Methods A **346** (1994) 461.
D. Buskulic *et al.* (ALEPH Collab.), preprint CERN-PPE/94-170, submitted to Nucl. Instrum. Methods A.

[11] D. Decamp *et al.* (ALEPH Collab.), Z. Phys. C **53** (1992) 1.

[12] D. Buskulic *et al.* (ALEPH Collab.), Phys. Lett. B **313** (1993) 535.

[13] D. Buskulic *et al.* (ALEPH Collab.), Phys. Lett. B **295** (1992) 174.

[14] D. Buskulic *et al.* (ALEPH Collab.), Phys. Lett. B **322** (1994) 275.

[15] T. Sjöstrand, Comp. Phys. Com. **82**, (1994) 74.
Throughout this analysis, a modified version of the JETSET 7.3 program was used to generate $Z \to q\overline{q}$ events. The Monte Carlo simulations take into account the performance characteristics of the ALEPH detector.

[16] D. Buskulic *et al.* (ALEPH Collab.), "Improved Measurement of the B_s^0 Lifetime with $D_s^- \ell^+$ Combinations," in preparation, to be submitted to Phys. Lett. B.

[17] L. Montanet *et al.* (Particle Data Group), Phys. Rev. D **50** (1994).

[18] D. Buskulic *et al.* (ALEPH Collab.), Phys. Lett. B **345** (1994) 103.

[19] D. Buskulic *et al.*, (ALEPH Collab.) "Measurements of the b Baryon Lifetime," submitted to Phys. Lett. B. In this paper branching fraction product is the sum of the electron and muon channels.

[20] The LEP collaborations and the LEP Electroweak Working Group, preprint CERN/PPE/94-187.

[21] J.R. Patterson, Proceedings of the XXVIIth International Conference on High Energy Physics, eds. P.J. Bussey and I.G. Knowles (IOP Publ. Ltd., Bristol, 1995), Vol. 1, p. 149.

[22] V. Sharma, "Recent Measurements of b Lifetimes," invited talk at the 6th International Symposium on Heavy Flavour Physics, Pisa, Italy, 6-10 June, 1995.

[23] D. Buskulic *et al.* (ALEPH Collab.), Phys. Lett. B **343** (1995) 444.

[24] C.G. Boyd, B. Grinstein and R.F. Lebed, preprint UCSD/PTH 95-03(1995).

[25] D. Buskulic *et al.* (ALEPH Collab.), Z. Phys. C **62** (1994) 179.